

Influence of tensor interactions on masses and decay widths of dibaryons

Hourong Pang

*Department of Physics, Nanjing University, Nanjing, 210093, P. R. China;
Institute of Theoretical Physics, Chinese Academy of Sciences, Beijing, 100080, China*

Jialun Ping

*Department of Physics, Nanjing Normal University, Nanjing, 210097, P.R. China;
Center for Theoretical Physics, Nanjing University, Nanjing, 210093, P.R. China*

Lingzhi Chen

Department of Physics, Nanjing University, Nanjing, 210093, China

Fan Wang

*Center for Theoretical Physics and Department of Physics,
Nanjing University, Nanjing, 210093, P. R. China*

T. Goldman

Theoretical Division, Los Alamos National Laboratory, Los Alamos, NM 87545, USA

Abstract

The influence of gluon and Goldstone boson induced tensor interactions on the dibaryon masses and D-wave decay widths has been studied in the quark delocalization, color screening model. The effective S-D wave transition interactions induced by gluon and Goldstone boson exchanges decrease rapidly with increasing strangeness of the channel. The tensor contribution of K and η mesons is negligible in this model. There is no six-quark state in the light flavor world studied so far that can become bound by means of these tensor interactions besides the deuteron. The partial D-wave decay widths of the $IJ^P = \frac{1}{2}2^+$ $N\Omega$ state to spin 0 and 1 $\Lambda\Xi$ final states are 12.0 keV and 21.9 keV respectively. This is a very narrow dibaryon resonance that might be detectable in relativistic heavy ion reactions by existing RHIC detectors through the reconstruction of the vertex mass of the decay product $\Lambda\Xi$ and by the COMPAS detector at CERN or at JHF in Japan and the FAIR project in Germany in the future.

PACS numbers: 12.39.-x, 14.20.Pt, 13.75.Cs

I. INTRODUCTION

There might be two kinds of dibaryon[1, 2]. One is the loosely bound type consisting of two octet baryons; the deuteron is a typical example. The others are tightly bound; the H particle had been predicted to be such a six quark state although later calculations cast doubt on it[3, 4]. Instead, a non-strange $IJ^p = 03^+$ d^* and a strangeness -6 $IJ^p = 00^+$ di- Ω have been predicted to be tightly bound six quark states, which are formed from decuplet baryons[2, 5, 6, 7, 8, 9]. The strangeness -3 $IJ^p = \frac{1}{2}2^+$ $N\Omega$ has also been predicted to be of the tightly bound type[4, 10, 11].

The tensor interaction due to π exchange plays a vital role in the formation of loosely bound deuteron. In the d^* case the tensor interaction contribution to its mass is minor but is critical for its D-wave decay to the NN final state[12]. There are other near threshold and deeply bound dibaryon candidates found in two systematic quark model calculations[4, 8]. This naturally raises the question as to whether or not the tensor interaction adds sufficient strength to bind these other near threshold states to become strong interaction stable, as in the deuteron case? Conversely, is the tensor interaction weak enough to leave the high spin, deeply bound states as narrow dibaryon resonances, as was shown in the d^* case[12]?

The present calculation is aimed at answering these two questions for the dibaryon candidates in the u,d,s three flavor world within the extended quark delocalization, color screening model (QDCSM). Our results show that both the effective S-D wave transition interactions due to gluon and π exchanges decrease rapidly with increasing strangeness, and that the tensor contributions of K and η mesons are negligible after a short range truncation. Altogether, the tensor contributions are not strong enough to bind other near threshold six quark states, such as the $SIJ^p = -401^+\Xi\Xi$, to become strong interaction stable with the sole exception of the deuteron. The D-wave decay widths of high spin, six quark states, such as the $SIJ^p = 003^+d^*$ and the $SIJ^p = -3\frac{1}{2}2^+N\Omega$, are in the range of tens of MeV to tens of keV and so these states might be narrow dibaryon resonances.

The extended QDCSM is briefly introduced in Section II. In Section III, we present our results. The discussion and conclusion are given in Section IV.

II. BRIEF DESCRIPTION OF THE EXTENDED QDCSM

The QDCSM was put forward in the early 90's. Details can be found in Refs.[2, 12, 13]. Although the short range repulsion and the intermediate range attraction of the NN interaction are reproduced by the combination of quark delocalization and color screening, the effect of the long-range pion tail is missing in the QDCSM. Recently, the extended QDCSM was developed[7], which incorporates this long-range tail by adding π -exchange but with a short-range cutoff to avoid double counting because the short and intermediate range interactions have been accounted for by the quark delocalization and color screening mechanism[14]. The exchange of K and η mesons has been shown to be negligible in this model approach[4, 9]. Nevertheless, their effect, especially the tensor part, has been included in this calculation to check further whether they are negligible in our model approach. The extended QDCSM not only reproduces the properties of the deuteron well, but also improves agreement with NN scattering data as compared to previous work[15].

The Hamiltonian of the extended QDCSM, wave functions and the necessary equations used in the current calculation are given below. The tensor interactions due to effective one gluon and the octet Goldstone boson exchanges are included. The details of the resonating-group method (RGM) have been presented in Refs.[12, 16].

The Hamiltonian for the 3-quark system is the same as the well known quark potential model, the Isgur model. For the six-quark system, we assume

$$\begin{aligned}
H_6 &= \sum_{i=1}^6 (m_i + \frac{p_i^2}{2m_i}) - T_{CM} + \sum_{i < j=1}^6 [V_{conf}(r_{ij}) + V_G(r_{ij}) + V_\pi(r_{ij})], \\
V_G(r_{ij}) &= \alpha_s \frac{\vec{\lambda}_i \cdot \vec{\lambda}_j}{4} \left[\frac{1}{r_{ij}} - \frac{\pi}{2} \delta(\vec{r}_{ij}) \left(\frac{1}{m_i^2} + \frac{1}{m_j^2} + \frac{4\vec{\sigma}_i \cdot \vec{\sigma}_j}{3m_i m_j} \right) + \frac{1}{4m_i m_j r_{ij}^3} S_{ij} \right], \\
V_\pi(r_{ij}) &= \theta(r - r_0) \frac{g_8^2}{4\pi} \frac{m_\pi^2}{4m_q^2} \frac{1}{r_{ij}} e^{-m_\pi r_{ij}} \left[\frac{1}{3} \vec{\sigma}_i \cdot \vec{\sigma}_j + Z(r_{ij}) S_{ij} \right] \vec{\tau}_i \cdot \vec{\tau}_j, \\
S_{ij} &= 3 \frac{\vec{\sigma}_i \cdot \vec{r}_{ij} \vec{\sigma}_j \cdot \vec{r}_{ij}}{r_{ij}^2} - \vec{\sigma}_i \cdot \vec{\sigma}_j, \\
Z(r) &= \frac{1}{3} + \frac{1}{m_\pi r} + \frac{1}{(m_\pi r)^2}, \\
V_{conf}(r_{ij}) &= -a_c \vec{\lambda}_i \cdot \vec{\lambda}_j \begin{cases} r_{ij}^2 & \text{if } i, j \text{ occur in the same baryon orbit,} \\ \frac{1-e^{-\mu r_{ij}^2}}{\mu} & \text{if } i, j \text{ occur in different baryon orbits,} \end{cases}
\end{aligned} \tag{1}$$

$$\theta(r_{ij} - r_0) = \begin{cases} 0 & r_{ij} < r_0, \\ 1 & \text{otherwise,} \end{cases}$$

where r_0 is the short range cutoff for pion exchange between quarks. g_8 is the π quark coupling constant. m_π is the measured π mass. The K and η meson exchange interactions, which have not been shown explicitly in the above equation but have been included in this calculation, have a form very similar to that for the π . The color screening constant, μ , is to be determined by fitting the deuteron mass in this model. All other symbols have their usual meanings, and the confinement potential $V_{conf}(r_{ij})$ has been discussed in Refs.[7, 12].

The pion exchange interaction, $V_\pi(r_{ij})$, affects only the u and d quarks. We take these to have a common mass, $m_q = m_d = m_u$, i.e., ignoring isospin breaking effects.

The quark wave function in a given nucleon (orbit) relative to a reference center (defined by \vec{S}) is taken to have a Gaussian form characterized by a size parameter, b ,

$$\phi(\vec{r} - \vec{S}) = \left(\frac{1}{\pi b^2} \right)^{3/4} e^{-\frac{1}{2b^2}(\vec{r} - \vec{S})^2}. \quad (2)$$

The light quark mass, m_q , is chosen to be $\frac{1}{3}$ of the nucleon mass. The strange quark mass, m_s , baryon size parameter, b , effective quark-gluon coupling constant, α_s , and the strength of confinement, a_c , are all determined by reproducing the nucleon mass, the $\Delta - N$ mass difference, an overall fit to other ground state baryon masses and by requiring the nucleon mass to be variational stable with respect to its size parameter, b . The quark-pion coupling constant $g_8 = g_{qq\pi}$ is obtained from the nucleon-pion coupling constant by a slight ($< 10\%$) correction to the classic symmetry relation, viz.,

$$\frac{g_{NN\pi}^2}{4\pi} = (M_N/m_q)^2 \left(\frac{5}{3} \right)^2 \frac{g_8^2}{4\pi} e^{m_\pi^2 b^2 / 2}, \quad (3)$$

where M_N is the nucleon mass and the last factor provides the correction due to the extent of the quark wavefunction in the nucleon. The K and η are assumed to have a flavor SU(3) symmetric quark-meson coupling constant and the same short range cutoff, r_0 , as the π 's. The color screening parameter, μ , has been determined by matching our calculation to the mass of the deuteron. All of the model parameters are listed in Table I.

Table I: Model Parameters

$m_q, m_s(MeV)$	$b(fm)$	$a_c(MeV \cdot fm^{-2})$	α_s	$\frac{g_8^2}{4\pi}$	$r_0(fm)$	$\mu(fm^{-2})$
313, 634	0.6022	25.03	1.5547	0.5926	0.8	0.90

The model masses of all octet and decuplet baryons are listed in Table II.

Table II: Single Baryon Masses in Units of MeV

	N	Σ	Λ	Ξ	Δ	Σ^*	Ξ^*	Ω
theor.	939.0	1217.5	1116.9	1357.6	1232.0	1359.6	1499.7	1652.3
expt.	939	1193	1116	1318	1232	1385	1533	1672

We use the RGM to carry out a dynamical calculation. The trial RGM di-baryon wave function is

$$\Psi(6q) = \mathcal{A} [\psi_{B_1}(\xi_1)\psi_{B_2}(\xi_2)]^{IS} \chi(\vec{R}), \quad (4)$$

where \mathcal{A} is the antisymmetrization operator, $\psi_{B_i}(\xi_i)$ $i = 1, 2$ is the baryon internal wave function including color-flavor-spin-orbital part, $[\dots]^{IS}$ means coupling the individual color-isospin-spin into the channel isospin-spin and overall color singlet.

To simplify the RGM calculation, one usually introduces Gaussian functions with different reference centers S_i $i=1\dots n$, which play the role of generating coordinates in this formalism, to expand the relative motion wave function $\chi(\vec{R})$ of the two quark clusters,

$$\chi(\vec{R}) = \left(\frac{3}{2\pi b^2}\right)^{3/4} \sum_i C_i e^{-\frac{3}{4}(\vec{R}-\vec{S}_i)^2/b^2}. \quad (5)$$

In principle, any set of base wave functions can be used to expand the relative motion wave function. The choice of a Gaussian with the same size parameter, b , as the single quark wave function given in Eq.(2), however, allows us to rewrite the resonating group wave function as a product of single quark wave functions; (see Eq.(6) below). This cluster wave function (physical basis) can be expressed in terms of the symmetry basis, classified by the symmetry properties in a group chain, which in turn allows the use of group theory method to simplify the calculation of the matrix elements of the six quark Hamiltonian[17]. In our calculations, we typically use 15 Gaussian functions to expand the relative motion wave function over the range 0-9 fm. For near threshold channels, such as the deuteron and H particle, more Gaussian functions are needed to extend the boundary to a larger extent to obtain more precise results as we have done previously. But in this calculation we did not make that effort because it is not necessary for our purpose.

After including the wave function for the six-quark center-of-mass motion, the ansatz for

the two-cluster wave function used in the RGM can be written as

$$\Psi_{6q} = \mathcal{A} \sum_{i=1}^n \sum_k \sum_{L_k=0,2} C_{i,k,L_k} \int d\Omega_{S_i} \prod_{\alpha=1}^3 \psi_R(\vec{r}_\alpha, \vec{S}_i, \epsilon) \prod_{\beta=4}^6 \psi_L(\vec{r}_\beta, \vec{S}_i, \epsilon) [[\eta_{I_{1k}S_{1k}}(B_{1k})\eta_{I_{2k}S_{2k}}(B_{2k})]^{IS_k} Y_{L_k}(\vec{S}_i)]^J [\chi_c(B_1)\chi_c(B_2)]^{[\sigma]}, \quad (6)$$

where k is the channel index. For example, for $SIJ = -2, 0, 0$, we have $k = 1, 2, 3$, corresponding to the channels $\Lambda\Lambda$, $N\Xi$ and $\Sigma\Sigma$. An angular momentum projection has been applied for the relative motion and L_k is the orbital angular momentum of the relative motion wave function of channel k .

The delocalized orbital wavefunctions, $\psi_R(\vec{r}, \vec{S}_i, \epsilon)$ and $\psi_L(\vec{r}, \vec{S}_i, \epsilon)$, are given by

$$\begin{aligned} \psi_R(\vec{r}, \vec{S}_i, \epsilon) &= \frac{1}{N(\epsilon)} \left(\phi(\vec{r} - \frac{\vec{S}_i}{2}) + \epsilon \phi(\vec{r} + \frac{\vec{S}_i}{2}) \right), \\ \psi_L(\vec{r}, \vec{S}_i, \epsilon) &= \frac{1}{N(\epsilon)} \left(\phi(\vec{r} + \frac{\vec{S}_i}{2}) + \epsilon \phi(\vec{r} - \frac{\vec{S}_i}{2}) \right), \\ N(\epsilon) &= \sqrt{1 + \epsilon^2 + 2\epsilon e^{-S_i^2/4b^2}}, \end{aligned} \quad (7)$$

where $\phi(\vec{r} - \frac{\vec{S}_i}{2})$ and $\phi(\vec{r} + \frac{\vec{S}_i}{2})$ are the single-particle Gaussian quark wave functions referred to above in Eq.(2), with different reference centers $\frac{S_i}{2}$ and $-\frac{S_i}{2}$, respectively. The delocalization parameter, ϵ , is a variational parameter determined by the dynamics of the quark system rather than being treated as an adjustable parameter. The initial RGM equation is

$$\int H(\vec{R}, \vec{R}') \chi(\vec{R}') d\vec{R}' = E \int N(\vec{R}, \vec{R}') \chi(\vec{R}') d\vec{R}'. \quad (8)$$

With the above ansatz, the RGM Eq.(8) is converted into an algebraic eigenvalue equation,

$$\sum_{j,k,L_k} C_{j,k,L_k} H_{i,j}^{k',L'_k,k,L_k} = E \sum_{j,k,L_k} C_{j,k,L_k} N_{i,j}^{k',L'_k,k,L_k} \delta_{L'_k, L_k}, \quad (9)$$

where $N_{i,j}^{k',L'_k,k,L_k}$, $H_{i,j}^{k',L'_k,k,L_k}$ are the wave function overlaps and Hamiltonian matrix elements, respectively, obtained for the wave functions of Eq.(6).

The partial width of a high spin dibaryon state decaying into a D-wave BB final state is calculated using Fermi's golden rule, in its nonrelativistic approximation, of course. Final state interactions have also been taken into account in our model approach[12]. The decay width formula used in $N\Omega \rightarrow \Lambda\Xi$ is a little different from that given in [12] due to the fact

that the decay products, Λ and Ξ , are different particles with different masses,

$$\Gamma(N\Omega \rightarrow \Lambda\Xi) = \frac{1}{2J+1} \sum_{M_{J_f}, M_{J_i}} \frac{1}{4\pi^2} p \frac{\sqrt{(m_\Lambda^2 + p^2)(m_\Xi^2 + p^2)}}{\sqrt{m_\Lambda^2 + p^2} + \sqrt{m_\Xi^2 + p^2}} \int |M_{fi}|^2 d\Omega, \quad (10)$$

$$p = \frac{\sqrt{(m_\Lambda^2 - m_\Xi^2)^2 + m_{N\Omega}^2(m_{N\Omega}^2 - 2m_\Lambda^2 - 2m_\Xi^2)}}{2m_{N\Omega}}.$$

III. RESULTS

Previously, we chose the di- Ω as an example to study whether or not our model results were sensitive to the meson-exchange cut-off parameter, r_0 , and the result demonstrated that they are not[9]. Hence, we consider it is sufficient to calculate six-quark systems of different quantum numbers with a representative cutoff value of $r_0 = 0.8 fm$. Table III displays the masses (in MeV) calculated for the dibaryon states of interest here. The deuteron channel result calculated previously is included in this table for comparison. It should be noted that in our calculation we assume the wavefunction to be zero at the boundary point, which is the usual boundary condition for bound states; i.e., we always solve the RGM Eq.(9) as an eigenvalue problem. If the state is unbound, we will not obtain a stable minimum eigenenergy in the course of extending the boundary point. Therefore the "mass" listed in Table III for these unbound states is not a true mass of a dibaryon state. However the contributions of tensor interaction are still a meaningful measure. The masses listed under the $Mass_{nt}$ and $Mass_{wt}$ are the calculated masses of those channels without and with tensor interaction.

Table III : Tensor Interaction Effect on the Masses of Six-Quark Systems

S,I,J	channel	$Mass_{nt}$	$Mass_{wt}$
0, 0, 1	NN	1880.295	1876.770(1880.250)
-2, 1, 1	$\Sigma\Sigma$	2418.686	2418.517
-3, 1/2, 1	$\Lambda\Xi$	2477.491	2477.488
-4, 0, 1	$\Xi\Xi$	2718.190	2718.189
-5, 1/2, 1	$\Xi\Omega$	3012.167	3012.140

The first line of Table III is the deuteron channel. If the tensor interaction is neglected the deuteron is unbound. Even if the tensor effect of gluon exchange is included, the deuteron

is still unbound. (The calculated mass is shown in parentheses). The tensor interaction due to π exchange is critical to form the actual stable deuteron and the η meson contribution is negligible. Fig. 1 shows the effective transition interactions of the NN S-D coupling due to gluon and π exchanges. The η contribution has not been shown because it is negligible. Obviously, the π contribution is dominant. The boundary point is limited to 9 fm and coupling to $\Delta\Delta$ channels has not been taken into account in this calculation; hence, the deuteron mass is a little higher than the best fit one which we reported previously. This weakness will not affect our conclusion regarding the tensor interaction effect mentioned above.

The $\Sigma\Sigma$ channel mass listed in the second line is lower than its own theoretical threshold 2435 MeV but higher than the $N\Xi$, $\Lambda\Sigma$ thresholds. A three S-wave channel coupling calculation has been done. The lowest mass is 2300 MeV which is still higher than the $N\Xi$ threshold and so can not form a narrow dibaryon resonance. The mass reduction due to the tensor interaction is very small as can be seen from Table III. Fig. 2 shows the S-D effective transition interactions in the $\Sigma\Sigma$ channel due to π , K and gluon exchange respectively. The π contribution is reduced by about a factor of four. The gluon contribution is also very much reduced. In addition, it is repulsive and cancels the π contribution. The K contribution is also repulsive and negligible. The η contribution is even smaller.

The $\Lambda\Xi$, $\Xi\Xi$, and $\Xi\Omega$ states are near threshold. The tensor interactions in these channels are much less effective than that in the deuteron channel and not strong enough to bind these baryons into dibaryon resonances. The mass reductions due to the tensor interactions in these channels are negligible as shown in Table III. Fig. 3 shows the S-D effective transition interactions in the $\Xi\Xi$ channel due to π , K and gluon respectively. The π contribution is reduced even further than in the previous case. The gluon contribution is very much reduced in comparison with that in deuteron channel but a little bit enhanced in comparison with that in $\Sigma\Sigma$ channel. The K contribution is further verified to be negligible and η negligible also.

Fig. 4 gives a direct comparison of the S-D effective transition interactions due to the tensor force of π exchange in NN, $\Sigma\Sigma$ and $\Xi\Xi$ channels. Fig. 5 gives a direct comparison of the S-D effective transition interactions due to the tensor force of gluon exchange in NN, $\Sigma\Sigma$, $\Lambda\Xi$, $\Xi\Xi$ and $\Xi\Omega$ channels. The η contribution has been calculated for all of these channels and all are negligible so they have not been shown explicitly.

As was mentioned in the introduction, the strangeness -3 $IJ^P = \frac{1}{2}2^+$ $N\Omega$ has also been predicted to be tightly bound[4, 10, 11] if the tensor interaction is neglected. Taking into account the tensor force, this state can couple to D-wave $\Lambda\Xi$ and $\Sigma\Xi$ channels. Since $\Lambda\Xi$ is the lowest channel in all channels with strangeness $S = -3$, here we only take into account this channel. For the possible $N\Omega(IJ = 1/2, 2)$ bound state we consider the two lowest $\Lambda\Xi$ D-wave decay channels: IS=1/2,0 and IS=1/2,1, respectively; here S specifies the channel spin. Such a tensor coupling has two effects: One is to modify the mass of the $N\Omega$ state; the other is to induce a transition from the $N\Omega$ to the D-wave $\Lambda\Xi$ final state and change the bound $N\Omega$ to a resonance with finite width. Both of these effects have been calculated.

The results show that, the mass of $N\Omega(IJ=1/2,2)$ in the single channel approximation is about 2566 MeV. Taking into account other S-wave channels coupling, such as $\Xi\Sigma, \Xi^*\Sigma, \Xi\Sigma^*, \Xi\Lambda$ and $\Xi^*\Sigma^*$, reduces the mass of the system to 2549 MeV, while adding the $\Lambda\Xi$ D-wave channel coupling only changes the value of mass slightly (not more than 1 MeV).

The widths of $N\Omega$ decays to the $\Lambda\Xi$ D-wave with different spins are listed in Table IV. For comparison, the width of the d^* decay to NN D-wave is also listed.

Table IV. Decay width. I,S,J are isospin, spin and total angular momentum, respectively.

$N\Omega(IJ = 1/2, 2) \rightarrow \Lambda\Xi$	$D - wave(S = 0, I = 1/2, J = 2)$	$\Gamma = 12.0 keV$
$N\Omega(IJ = 1/2, 2) \rightarrow \Lambda\Xi$	$D - wave(S = 1, I = 1/2, J = 2)$	$\Gamma = 21.9 keV$
$d^*(IJ = 0, 3) \rightarrow NN$	$D - wave(S = 1, I = 0, J = 3)$	$\Gamma = 6.57 MeV$

From Table IV we see that the width of d^* decay to the NN D-wave is 6.57 MeV. Comparison with our previous results[18], confirms that the width is not sensitive to the value of cutoff r_0 . The width of $N\Omega$ decays to $\Lambda\Xi$ D-wave is about tens of keV, about three orders of magnitude smaller. The result is not changed significantly for decay channels with different spin. For example, the $N\Omega \rightarrow \Lambda\Xi$ (spin=0) D-wave decay width is calculated to be 12.0 keV, and the $N\Omega \rightarrow \Lambda\Xi$ (spin=1) D-wave decay width is 21.9 keV. These results confirm our expectation that the $N\Omega$ is a narrow dibaryon resonance. (The width of $N\Omega \rightarrow \Lambda\Xi$ is smaller than that of the $d^* \rightarrow NN$ decay mainly due to the reduction of the tensor interaction, but also due to the fact that the N and Δ have the same flavor content while N, Ω and Λ , Ξ have differing flavor content in each baryon.)

IV. DISCUSSION AND CONCLUSION

The effects of the tensor interactions of gluon and Goldstone boson exchanges on the dibaryon mass and decay width have been studied in the extended QDCSM. Only in the deuteron channel is the tensor interaction of π exchange strong enough to bind the two nucleons into a loosely bound state. No other near threshold six-quark state studied so far in the u, d, s three flavor world can be bound together by the additional attraction induced by these tensor interactions. The S-D wave effective transition interactions due to π and gluon tensor forces both decrease rapidly with increasing strangeness. In the $\Sigma\Sigma$ and $\Xi\Xi$ channels the effective transition interactions due to the gluon tensor term become repulsive and cancel the attractive π contribution. The tensor contribution of explicit K and η meson is confirmed as negligible due to the same short range truncation as for the π , in our model approach[4, 9]

The mass shift of the $IJ^p = \frac{1}{2}2^+$ $N\Omega$ state induced by the tensor interaction is small (not more than 1 MeV) and the D-wave partial decay widths to $\Lambda\Xi$ with spin-0 and spin-1 are only 12.0 and 21.9 keV, respectively. Hence, the $IJ^p = \frac{1}{2}2^+$ $N\Omega$ state appears to be a good candidate for a narrow dibaryon resonance. Altogether there are only two promising narrow dibaryon resonances in the light flavor world in our model approach: The $IJ^p = 03^+ d^*$ and the $IJ^p = \frac{1}{2}2^+$ $N\Omega$.

The H particle and di- Ω are marginally strong interaction stable in our model. However the theoretical binding energies of both are small (only few MeV[4, 9]). Table II shows that the calculated ground octet and decuplet baryon masses deviate from the measured ones about 18 MeV on average. A reasonable estimate of the model uncertainty for the dibaryon mass would be at least that large. Therefore, in our model, it is unjustified to assert that the H particle and di- Ω might be strong interaction stable dibaryon candidates. This estimation is consistent with the latest di- Λ hypernuclear findings[19]. There are various broad resonances with widths $\sim 150 \rightarrow 250$ MeV around the d^* mass (~ 2180 MeV) in our model which makes the analysis of the NN scattering more difficult in the energy region $2.1 \rightarrow 2.4$ MeV where a broad bump has been found in the pp and np total cross sections. We will report on those results later. The $SIJ = -3, 1/2, 2$ $N\Omega$ state is quite convincingly lower in mass than the $N\Omega$ threshold, and quite possibly lower than the $\Lambda\Xi\pi$ threshold, as well. We have shown the decay width to be as small as tens of keV. Such a narrow

dibaryon resonance might be detected by reconstructing the invariant mass of its two body decay products, Λ and Ξ , in high Ω production reactions using RHIC at Brookhaven and COMPASS at CERN and the future ones at JHF in Japan and FAIR in Germany.

This model, the extended QDCSM, which proposes a new mechanism to describe the NN intermediate range attraction instead of the σ meson, well describes, with the fewest parameters, the properties of the deuteron and the existing NN, N Λ and N Σ scattering data. Up to now, it is the only model which gives an explanation of the long standing fact that the nuclear and molecular forces are similar in character despite the obvious length and energy scale differences and that nuclei are well described as collection of A nucleons rather than 3A quarks. In view of the fact that the H particle has not been observed experimentally, the BB interaction in the $\Lambda\Lambda$ channel[19] predicted by this model may be a good approximation of the real world. Based on these facts we suppose the predictions about dibaryon states of this model might also be approximately correct. Of course, the QDCSM is only a model of QCD. The high spin, high strangeness dibaryon resonance, $IJ^P = \frac{1}{2}2^+$ N Ω , may be a good venue to search for new hadronic matter and to test whether or not the QDCSM mechanism for the intermediate range attraction is realistic.

This work is supported by NSFC contracts 90103018 and 10375030. and by the U.S. Department of Energy under contract W-7405-ENG-36. F. Wang would like to thank the ITP for their support through the visiting program.

- [1] F. Wang, J.L. Ping and T. Goldman, *in* AIP conference Proceedings 338, ed. S.J.Seestrom, AIP Press, Woodbury, New York, 1995, p.538.
- [2] F. Wang *et al.*, Phys. Rev. **C51**, 3411 (1995).
- [3] R.L. Jaffe, Phys. Rev. Lett. **38**, 195 (1977).
R.L. Jaffe and F. Wilczek, Phys. Rev. Lett. **91**, 232003 (2003). hep-ph/0307341.
- [4] H.R. Pang *et al.*, nucl-th/0306043.
- [5] T. Goldman *et al.*, Phys. Rev. **C39**, 1889 (1989).
- [6] T. Goldman, *et al.*, Mod. Phys. Lett. **A13**, 59 (1998).
- [7] J.L. Ping, H.R. Pang, F. Wang and T. Goldman, Phys. Rev **C65**, 044003 (2002).
- [8] Q.B. Li *et al.*, Nucl. Phys. **A683**, 487 (2001).

- [9] H.R. Pang, J.L. Ping, F. Wang and T. Goldman, Commun. Theor. Phys. **38**, 424 (2002); Phys. Rev. **C66**, 025201 (2002).
- [10] T. Goldman *et al.*, Phys. Rev. Lett. **59**, 627 (1987).
- [11] H.R. Pang *et al.*, Commun. Theor. Phys. **41**, 67 (2004).
- [12] J.L. Ping, F. Wang and T. Goldman, Nucl. Phys. **A688**, 871 (2001).
- [13] F. Wang, G.H. Wu, L.J. Teng and T. Goldman, Phys. Rev. Lett. **69**, 2901 (1992).
- [14] H.R. Pang, J.L. Ping, F. Wang and T. Goldman, Phys. Rev. **C65**, 014003 (2001).
- [15] X.F. Lu, J.L. Ping and F. Wang, Chin. Phys. Lett. **20**, 42 (2003).
- [16] A.J. Buchmann, Y. Yamauchi and A. Faessler, Nucl. Phys. **A496**, 621 (1989).
- [17] F. Wang, J. L. Ping and T. Goldman, Phys. Rev. **C51**, 1648 (1995).
- [18] J.L. Ping, F. Wang and T. Goldman, Phys. Rev. **C62**, 054007 (2000).
- [19] H. Takahashi *et al.*, Phys. Rev. Lett. **87**, 212502 (2002).

FIGURE CAPTIONS

Fig.1 The effective S-D wave transition interactions of gluon and π tensor force in the deuteron channel.

Fig.2 The effective S-D wave transition interactions of gluon and π , K tensor force in the $IJ^P = 11^+$ $\Sigma\Sigma$ channel.

Fig.3 The effective S-D wave transition interactions of gluon and π , K tensor force in the $IJ^P = 01^+$ $\Xi\Xi$ channel.

Fig.4 A comparison of effective S-D wave transition interactions of π tensor force in NN, $\Sigma\Sigma$, $\Xi\Xi$ channels.

Fig.5 A comparison of effective S-D wave transition interactions of gluon tensor force in NN, $\Sigma\Sigma$, $\Lambda\Xi$, $\Xi\Xi$, $\Xi\Omega$ channels.

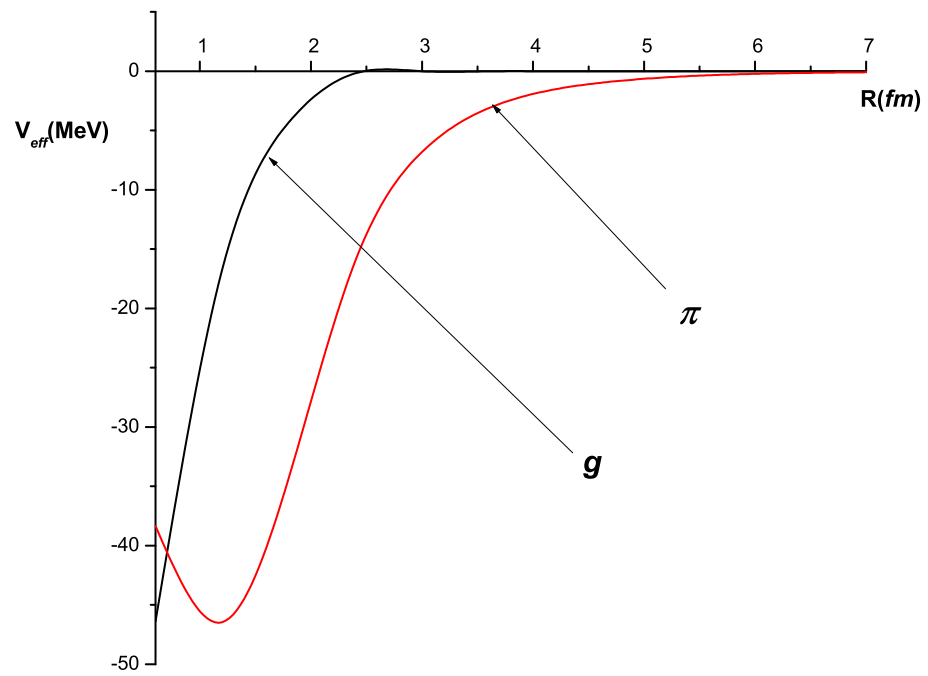


FIG. 1: The effective S-D wave transition interactions of gluon and π tensor force in the deuteron channel.

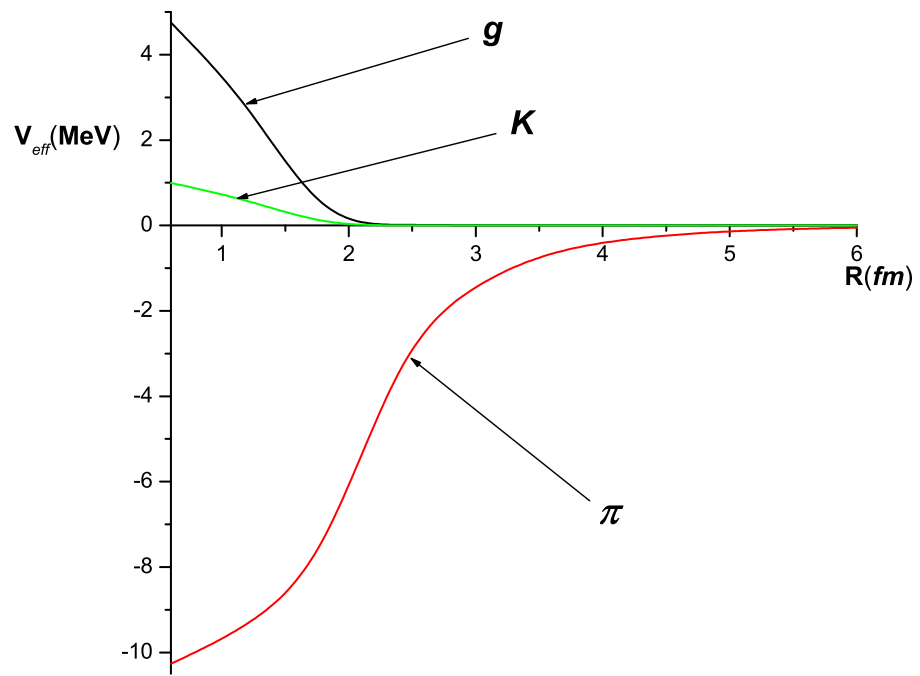


FIG. 2: The effective S-D wave transition interactions of gluon and π , K tensor force in the $IJ^p = 11^+ \Sigma\Sigma$ channel.

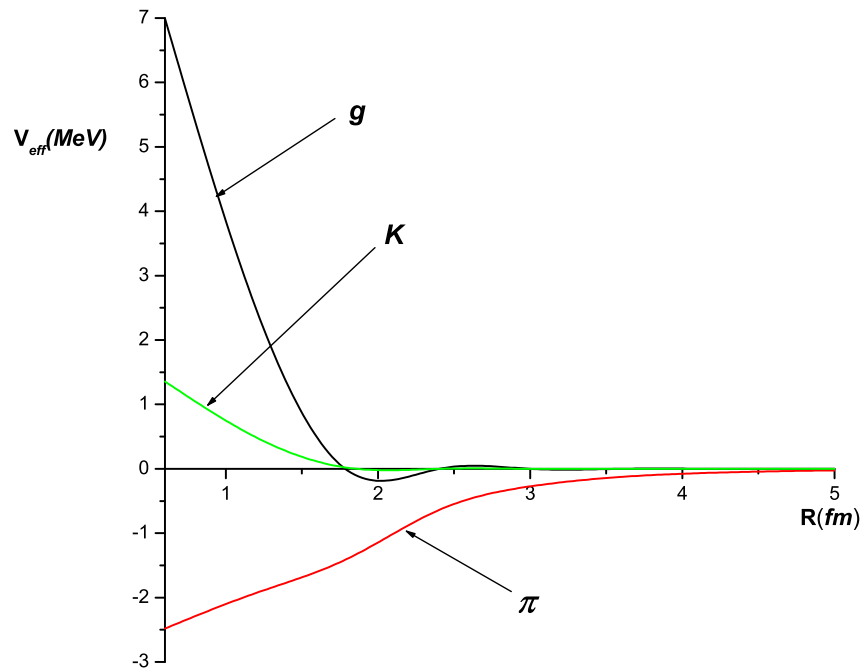


FIG. 3: The effective S-D wave transition interactions of gluon and π , K tensor force in the $IJ^p = 01^+ \Xi\Xi$ channel.

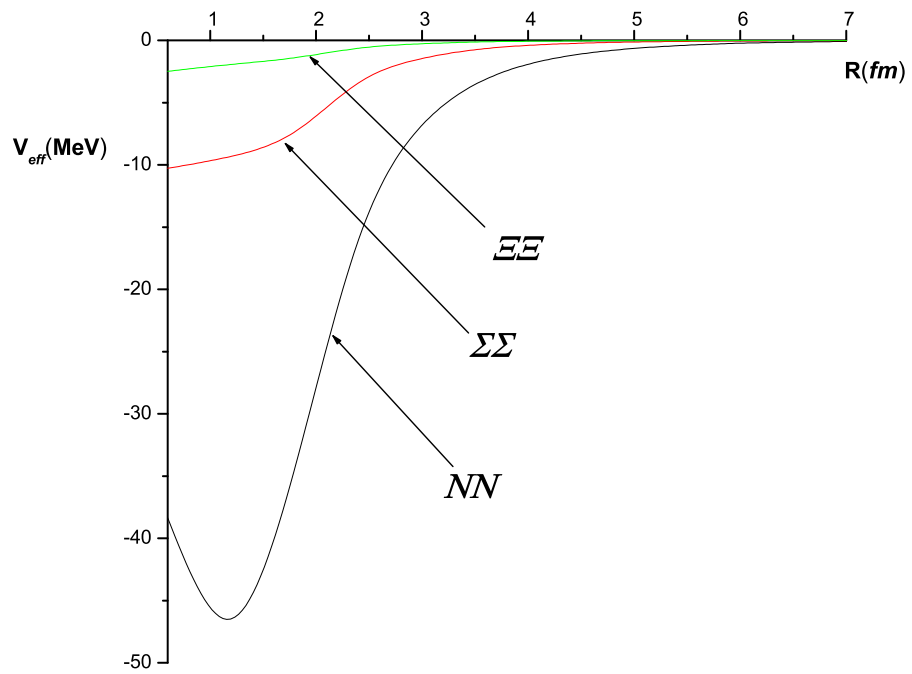


FIG. 4: A comparison of effective S-D wave transition interactions of π tensor force in NN , $\Sigma\Sigma$, $\Xi\Xi$ channels.

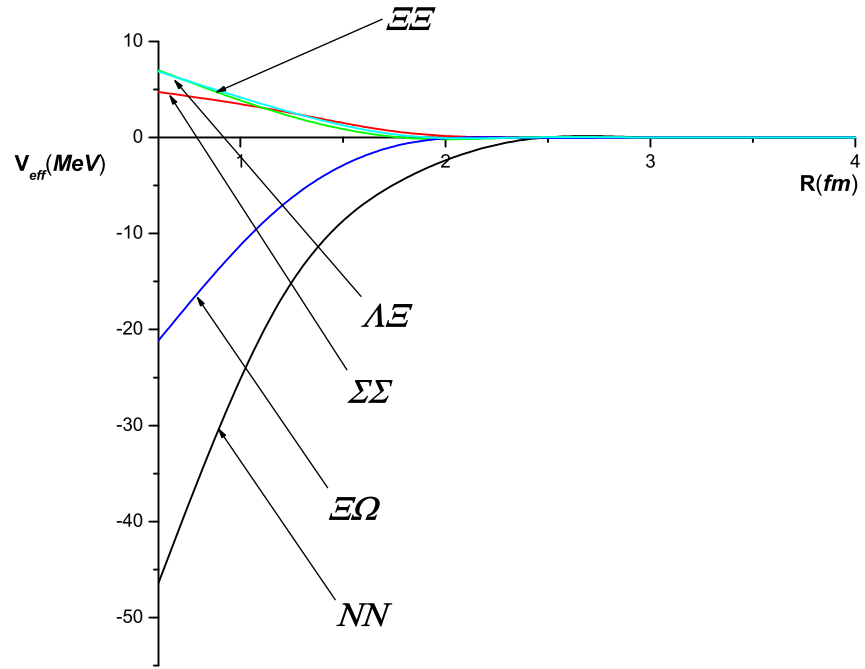


FIG. 5: A comparison of effective S-D wave transition interactions of gluon tensor force in NN, $\Sigma\Sigma$, $\Lambda\Xi$, $\Xi\Xi$, $\Xi\Omega$ channels.